Study on Numerical Simulation for Component Transportation and Oil Displacement of a Microbial System

Zhao Yang, Guo Zhihua, Jingchun Wu,* Shi Fang, Hanwen Zhang, and Zhang Miaoxin

Read Online

ACCESS | Metrics & More | Article Recommendations

ABSTRACT: Component transportation is one of the main mechanisms for numerical simulation in microbial oil recovery. However, the research on the component transportation considering the inhibition of metabolites is very limited. A mathematical model of oil displacement in a microorganism system including microbial growth and metabolism equation, component transport equation, and porous media physical property variation equation was established in this paper. The equation was discretized and solved by implicit pressure and explicit saturation. The MATLAB simulation results showed that the chromatographic separation between microorganisms and nutrients happened because of the adsorption of porous media and the activity of microorganisms during the transportation, and the separation degree of the chromatography became higher as the permeability became lower and the injection speed became slower. The multislug alternative injection mode could reduce the degree of chromatographic separation, and the recovery rate can be increased to 50.82%. The results of this study could provide theoretical guidance for the popularization and application of microbial enhanced oil recovery (MEOR).
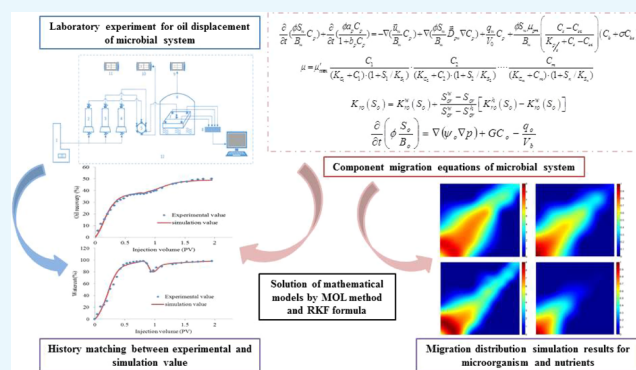
1. INTRODUCTION

For the first time, Beckman proposed an idea that using microbial self-activities and metabolism to improve oil recovery in 1926 till now, the application of microbial enhanced oil recovery technology is becoming more and more extensive.[1,2] Microbial enhanced oil recovery (MEOR) is an alternative tertiary oil recovery technology where microbial metabolites (biomass,[3] biopolymers,[4] gases, acids, solvents, enzymes, and surface-active compounds[5]) and activities (hydrocarbon metabolism, plugging) are used to improve the recovery of residual oil from depleted and marginal reservoirs.[6,7]

Numerical simulation for reservoirs has the advantages of simple operation and low cost. On the basis of mutual verification of laboratory experiments, the risk of oil field development can be greatly reduced, the development plan can be optimized, and an important basis for field test can be provided.[8,9] The premise of numerical simulation of microbial enhanced oil recovery is the establishment of mathematical equations. Since the 1980s, foreign scholars have begun to establish mathematical models related to microbial enhanced oil recovery and have developed these rapidly. Knapp established a mathematical model for microbial flooding based on the microbial growth and metabolic control equations.[10] Islam had considered the applicability of a microbial reservoir in establishing mathematical models. Based on the experiment of microbial porous medium

migration, Chang established a mathematical model considering microbial growth, extinction, and adsorption. Zhang considered the consumption of nutrients and the formation of metabolites in the mathematical model of convection diffusion.[11] The establishment of these models is the basis for the numerical simulation of microbial enhanced oil recovery.[12,13]

The Islam, Zhang, and Chang models were added to different microbial growth and metabolic control equations on the basis of commonly used black oil models and component models. But these three models simply describe the biological activity and the impact on oil displacement. Most scholars later revised and perfected them on the basis of these three models.[14] Delshad established a mathematical model of microbial growth kinetics with various factors. On this basis, a complex oil displacement mathematical model considering the effects of the biosurfactant, biopolymer, and biogenic gas was established. The effect of metabolites was related to the
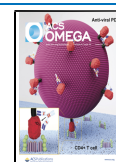
flooding mechanism of chemical agents in chemical flooding. Sivasankar established a coupled mathematical model of temperature field, injection speed, and microbial kinetics parameters to characterize the microbial flooding process.[15] On the basis of previous studies, the model put forward two parameters, namely, the amount of nutrient needed by the strain itself and the amount of nutrients needed to produce the surfactant. By solving the mathematical model, the results are compared with the indoor physical simulation experiments and the existing model calculation results. It was better to verify the comparison result. Hosseininoosheri used UTCHEM to establish a 3D model for the surfactant flooding process.[16] The model mainly studied the effects of temperature, salinity, and pH on the growth rate of microbial strains.

Although a great deal of research has been done on microbial oil recovery, there are certain differences among mathematical models. In the microbial growth and metabolism model, the restriction of nutrients is considered more, and the inhibition of metabolites is less. In this paper, the equations of microbial growth and metabolism, the transport equations of microbial components, and the equation of physical change properties in porous media have been established. The mathematical equations are discretized by the finite difference method, and the numerical simulation results are verified with laboratory experiments. Bacteria CBS-2 and WBP-1 have been used in laboratory oil displacement experiments. CBS-2 is a *Pseudomonas* sp., and the product is a biosurfactant. WBP-1 is an *Agrobacterium*, and the product is a biopolymer. The combination of bacteria CBS-2 and WBP-1 has a synergistic oil displacement effect. Then, the distribution rule of each component of the microbial system is described, and the displacement effect of different development schemes are compared and analyzed.

2. RESULTS AND DISCUSSIONS

2.1. Model Verification Results. Figures 1 and 2 are the dynamic change curves of recovery and water content.
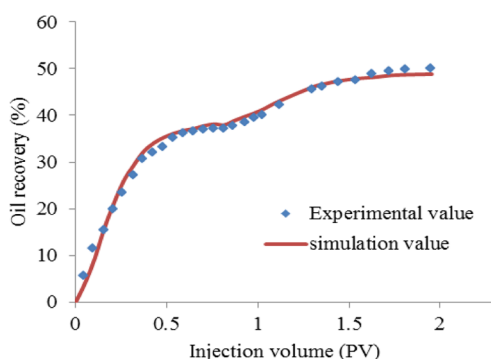
Figure 1. History matching between the experimental and simulation value.

Compared with the experimental and numerical simulation results, it can be observed that the numerical simulation results are close to the experimental value. The recovery degree of the water flooding simulation stage is 37.96%, the experimental value is 37.24%, and the relative error is 1.93%. The recovery degree of the microbial flooding simulation stage is 3.51%, the experimental value is 3.42%, and the relative error is 2.34%. The total recovery rate of the numerical simulation and experiment is 48.85 and 50.16% respectively, and the relative
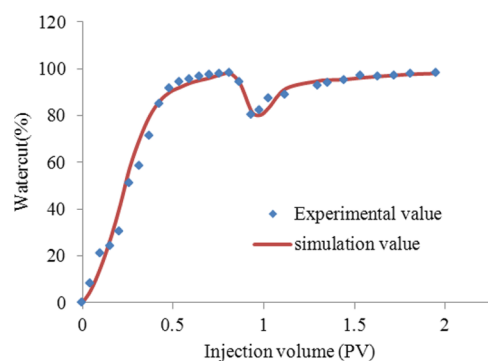
**Figure 2.** History matching between the experimental and simulation value.

error is 2.61%. The results show that the established model for microbial enhanced oil recovery could better simulate the actual situation.

2.2. Influence of Permeability on Component Distribution. The number of model grids was 40×40, the grid length was 5 m, and the time step was 1 month. The well pattern adopted a five-point well pattern that had one injection well and four production wells. The injection system selected was the CBS-2 and WBP-1 composite system, the compound ratio was 1:1, the injection concentration was 10^5/mL, the injection volume was 0.2 PV, and the injection speed was 0.1PV/a. The distributions of microorganisms and nutrients were simulated under different permeability (50, 100, and 300 $\times 10^{-3}$ μm^2) conditions.
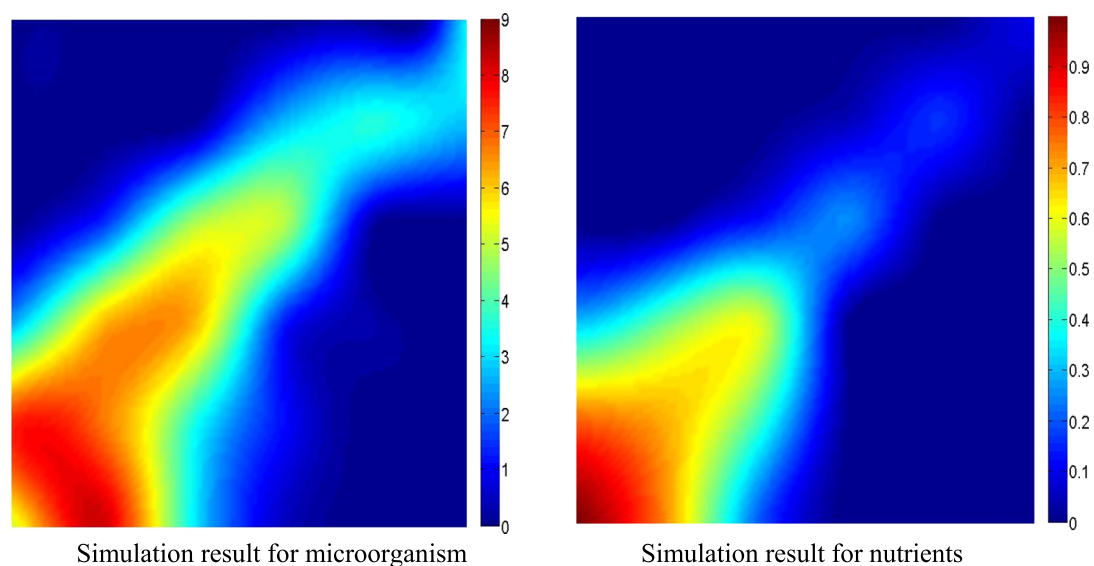
The results of distribution simulation showed that the microorganisms and nutrients in the microbial system had a chromatographic separation phenomenon similar to chemical flooding. After injecting the microbial system into the reservoir, microorganisms grew and propagated rapidly near the injection well due to the high concentration of nutrients, and the concentration of microorganisms was rising. During the process of microbial flooding, the nutrients were gradually reduced by the consumption of microbes and the adsorption of pore, and then the growth rate of microorganisms was reduced. When the growth rate was lower than the decay rate, the concentration of microorganisms began to decrease. Therefore, the nutrients were almost depleted and the concentration of microorganisms was less than 10^4 /mL near the production well (Figures 3−5).

Compared with the system distribution results under different permeability conditions, the chromatographic separation degree of microorganisms and nutrients was higher when the permeability was lower under the same injection volume. This is because the lower the permeability was, the larger the specific surface area of the rock pores was, and so the amount of adsorption for nutrients was increased.[17] As shown in Figure 6, when the nutrient concentration was half of the initial injection during the flooding process, the systems moved into 102, 125, and 178 m, respectively in 50, 100, and 300 $\times$ 10^{-3} μm^2 models.

2.3. Influence of Injection Speed on Component Distribution. The permeability of the model was 100×10^{-3} μm^2, the injection system was selected by the microorganism compound system, the compound ratio of CBS-2 and WBP-1 was 1:1, the injection concentration was 10^5/mL, the injection volume was 0.2 PV, and the microorganisms and nutrients

Simulation result for microorganism

Simulation result for nutrients
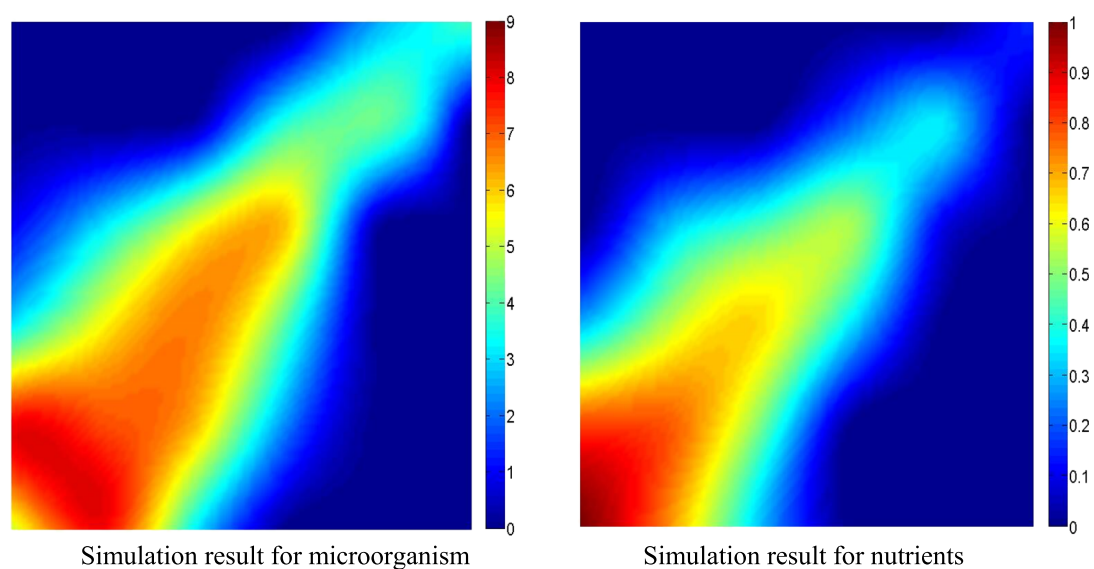
Figure 3. Migration distribution simulation results for microorganisms and nutrients (300×10^{-3} μm^2).

Simulation result for microorganism

Simulation result for nutrients

Figure 4. Migration distribution simulation results for microorganisms and nutrients (100×10^{-3} μm^2).

were distributed under the conditions of different (0.1, 0.15, and 0.2 PV/a) injection speeds.

Simulation results of Figures 7−9 showed that the higher the injection speed was, the lower was the chromatographic separation degree between microorganisms and nutrients. This is because the increase of the velocity of the fluid increased the driving force of the fluid on the nutrients, thereby reducing the adsorption of the pores on the nutrients, increasing the transmission capacity of the nutrients, and keeping the microbes' high growth rate for a long time during the migration process. However, the high injection speed increased the fingering phenomenon of the system and reduced the sweep area of the system.

When chromatographic separation between microorganisms and nutrients occurred, the ability of microorganisms to grow and metabolize was low because fewer nutrients could be absorbed by the microorganisms at the tip of the displacement fluid. Furthermore, it affected the development effect of the reservoir. Therefore, a certain amount of nutrient solution

should be injected into the reservoir before the injection of the microbiological system. This method could not only reduce the absorption of nutrients in the subsequent microorganism system but also provide energy for the microbe in the process of migration so that the microorganism can maintain good growth and metabolism in the porous medium. In addition, the injection speed of the system can be increased to further reduce the chromatographic separation.

2.4. Influence of Different Programs on Oil Recovery. The production dynamics of three different injection modes were simulated. The time step was 1 month, and the injection speed was 0.15 PV/a. Scheme I: water flooding; Scheme II: after injection water until the water cut was 98%, the microbial system was injected, and the injection volume was 0.2PV, followed by water flooding to 98% of water content; Scheme III: after water flooding to 98% of water content, nutrient substance system was injected, injection volume was 0.1 PV, then the microorganism system was injected, injection volume was 0.2 PV, follow up injected with 0.1 PV nutrient substance

Simulation result for microorganism   Simulation result for nutrients
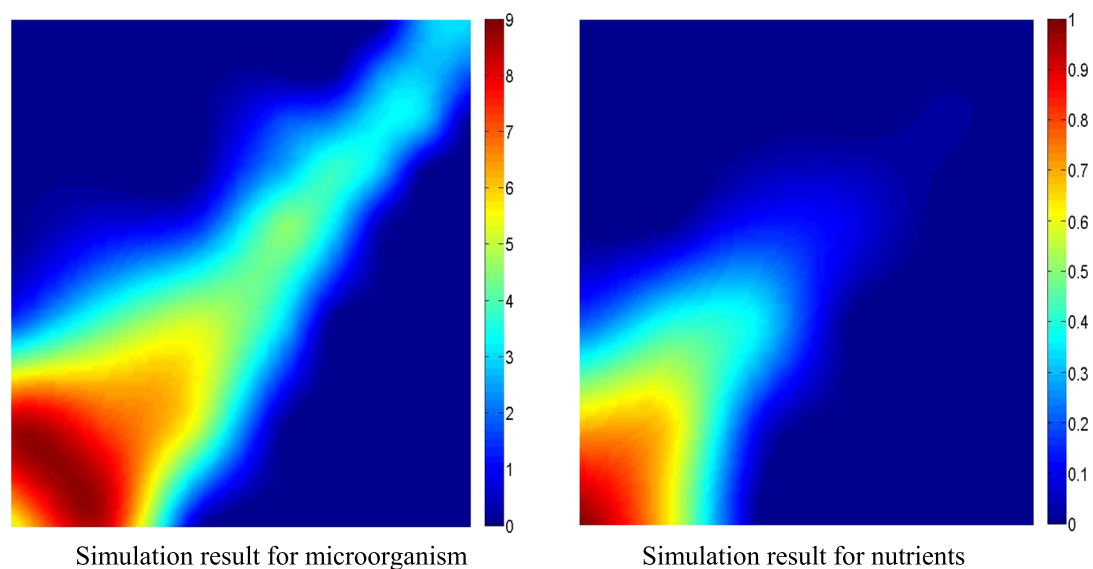
Figure 5. Migration distribution simulation results for microorganisms and nutrients $(50 \times 10^{-3}\ \mu m^2)$.
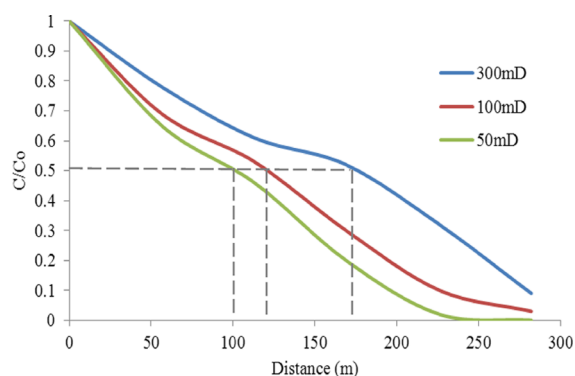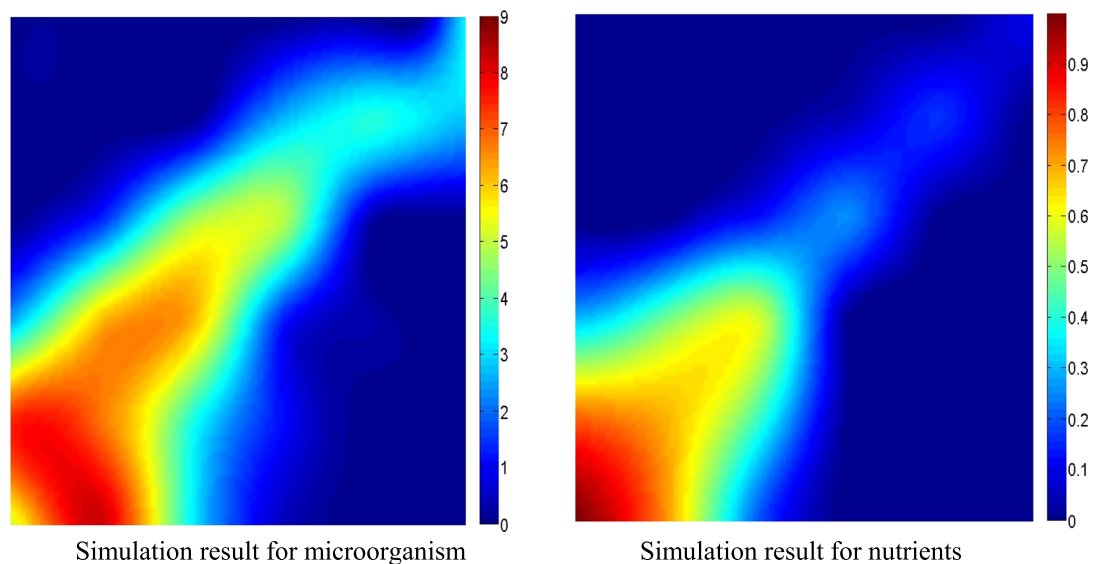

Figure 6. Migration distribution of nutrients under different permeability.

system, followed by water flooding to 98% of water cut; Scheme IV: using multislug injection system as: water flooding

to water content 98% + 0.05 PV nutrient substance system + 0.05 PV microbial system + 0.05 PV nutrient substance system + 0.05 PV microbial system + 0.05 PV nutrient system + 0.05 PV nutrient system + 0.05 PV system + 0.05 PV nutrient system + 0.05 PV microbial system + follow water flooding to 98% water cut. The simulation results are shown in Table 1 and Figures 10 and 11.

Comparing the dynamic curves of oil recovery and water cut in different injection schemes, it was showed that scheme IV that used multislug injection had the best effect of enhanced oil recovery. The total recovery rate of scheme IV was 50.82%, which was 12.86% higher than that of water flooding recovery, and the recovery rate after measures increased by 1.97 and 1.13%, respectively, compared with schemes II and III.

Before injecting the microorganism system, nutrients were firstly injected, and it could slow down the chromatographic separation between nutrients and microorganisms in the microbial system. At the same time, the subsequent

Simulation result for microorganism   Simulation result for nutrients

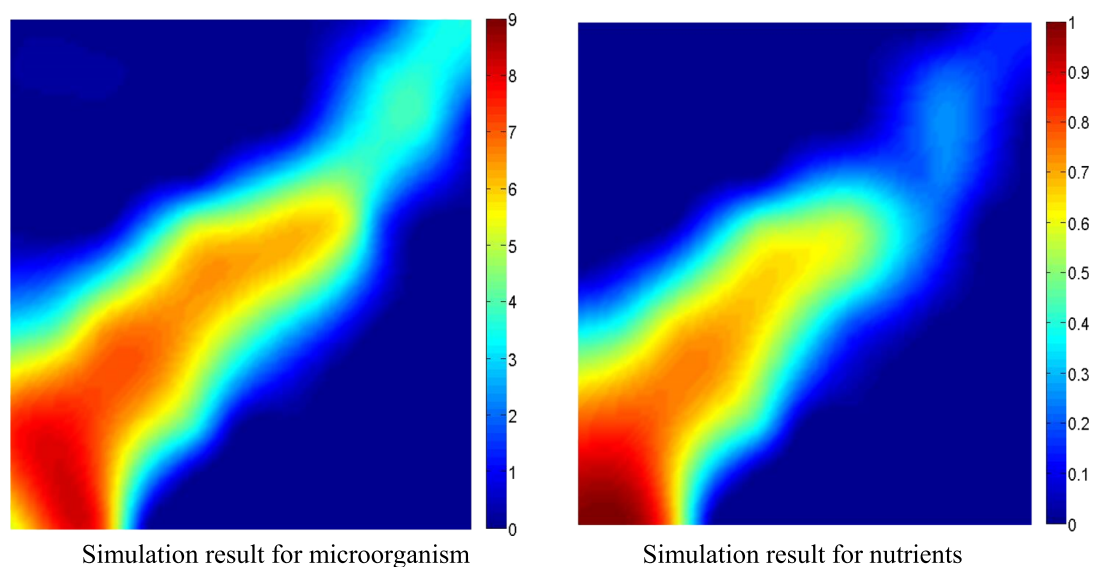**Figure 7.** Migration distribution simulation results for microorganisms and nutrients (0.1 PV/a).

Simulation result for microorganism   Simulation result for nutrients

Figure 8. Migration distribution simulation results for microorganisms and nutrients (0.15 PV/a).

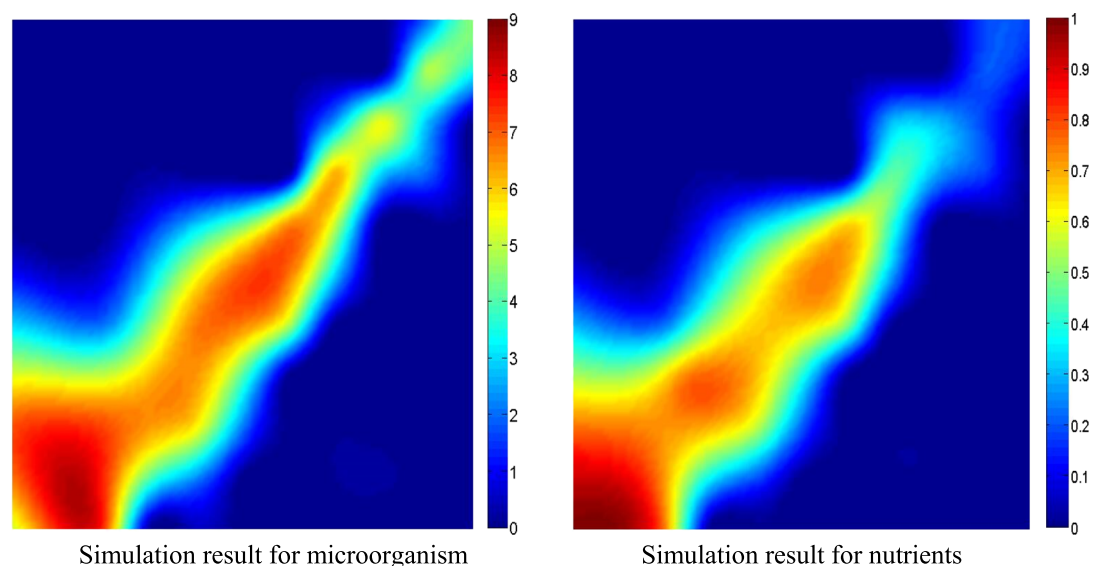Simulation result for microorganism   Simulation result for nutrients

Figure 9. Migration distribution simulation results for microorganisms and nutrients (0.2 PV/a).

Table 1. The Oil Recovery Change of Different Injection Modes

scheme	water flooding recovery rate (%)	improvement of recovery rate after measures (%)	total recovery rate (%)
I	37.96		37.96
II	37.96	10.89	48.85
III	37.96	11.73	49.69
IV	37.96	12.86	50.82

supplementation of nutrients promoted the growth and metabolism of microorganisms in porous media. Therefore, the recovery rate of scheme III was higher than that of scheme II. But scheme III was a one-time injection for prenutritive material slug. With the injection of the follow-up system, a part of nutrients in the front slug would be picked up before contacting with microorganisms. Therefore, on the basis of scheme III, scheme IV used a multislug alternative injection to reduce the loss of prenutrient substances and made the microbes contact more nutrients in the process of migration in
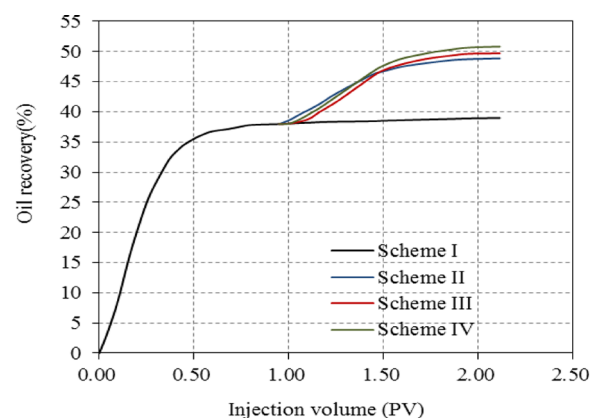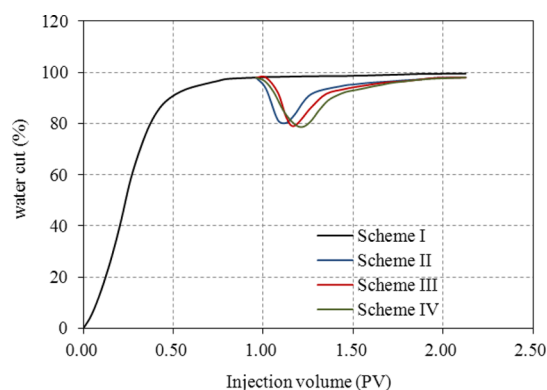

Figure 10. Total oil recovery curves under different injection schemes.

Figure 11. Water cut and oil recovery curves under different injection schemes.

the porous medium, especially near the product wells, so it could make microorganisms keep good growth and metabolism ability and enhanced the displacement effect.

3. CONCLUSIONS

(1) A mathematical model of the microbial system for oil displacement was established, including the equation of microbial growth and metabolism considering the restriction of nutrient substance; the migration equation of each component considering the factors of adsorption, retention, and tendency; as well as the equation of physical properties of porous media considering porosity, permeability, interfacial tension, viscosity, and so on. The equation is discretized and solved by implicit pressure and explicit saturation.

(2) The phenomenon of chromatographic separation occurred when microorganisms and nutrients migrated in porous media. Nutrient contents gradually decreased due to the consumption of microorganisms and the adsorption of pores. Therefore, the growth rate of microorganisms was reduced, and near the production well, nutrients were almost depleted; the microbial concentration was lower than 10^4/mL.

(3) The lower the permeability was, the greater the specific surface area of the rock pores was, the stronger the adsorption of nutrients by the pores was, and the higher the chromatographic separation degree between microorganisms and nutrients was. Increasing the injection speed could slow down the chromatographic separation between microorganisms and nutrients. At the same time, it also aggravated the phenomenon of fingering and reduced the swept area of the system.

(4) The results of indoor physical simulation and numerical simulation were verified well. It showed that the numerical simulation results were close to the experimental values. And the relative error of recovery degree and total recovery was less than 4%. The established microbial system oil displacement model can simulate the actual situation well.

(5) The numerical simulation results under different development schemes showed that the injection with multislug had the best recovery, and the total recovery was 50.82%, which was 12.86% higher than that of water flooding recovery.

4. METHODOLOGY

The transport equations of microorganisms, nutrients, and metabolites were established by means of material balance in this paper, and the mathematical models for microbial oil recovery considering various factors were established combining microbial growth kinetics equation and physical property variation equation in porous media. The finite difference method was used to discretize the equations, and then the mathematical models were solved by implicit pressure and explicit saturation.

In the process of establishing the mathematical models, some conditional assumptions were needed to facilitate the solution, as follows: There were two phase fluids (oil and water) in porous media, while microorganisms, nutrients, and microbial metabolites only existed in the water phase. The flow of oil and water phase both followed Darcy's law. Reservoir rock and fluid were weak compressible. The adsorption and desorption process of microorganisms was carried out on the rock surface at the same time, and the adsorption of nutrients and metabolites conformed to Langmuir isothermal adsorption. Metabolites such as the biosurfactant affected the growth rate of microorganisms, while biofilms could reduce reservoir permeability. The reservoir temperature remained stable.

4.1. Component Migration Equations of Microbial System. The migration of microorganisms in porous media was mainly affected by capillary force, dispersion force, and viscous force.[18] According to the equation of matter equilibrium, the migration equations of microorganisms could be written as:

$$\frac{\partial}{\partial t}\left(\frac{\phi S_w}{B_w}C_b\right) + \frac{\partial}{\partial t}(\phi C_{bs})$$
$$= -\nabla\left(\frac{\vec{u}_b}{B_w}C_b\right) + \nabla\left(\frac{\phi S_w}{B_w}\vec{D}_{bw}\nabla C_b\right) + \frac{q_w}{V_0}C_b + \frac{\phi S_w}{B_w}v_b$$

$$(1)$$

The first item on the left represented the concentration change of microbes in the water phase, and the second item represented the adsorption change of microbes in the porous media. The first item on the right was the convective phase of the microorganism, the second item was the diffusion phase, the third item was the injection or extraction phase, and the last item was the phase of the growth and decline of the microorganism.

C_b was the concentration of microorganisms in the water phase; C_{bs} was concentration of microbes in the attached phase; $\vec{u}_b$ was the total velocity for microorganisms; $\vec{D}{\rightharpoonup}_{bw}$ was the physical dispersion tensor for microorganisms in the water phase; v_b was the growth and decay rate; ϕ was the porosity; S_w was the saturation for the water phase; B_w was the formation volume factor; q_w was volumetric injection or extraction rate for the water phase; and V_0 was the rock bulk volume.

The total velocities for microorganisms included the Darcy velocity of the water phase and the self-motion velocity of microorganisms:

$$\vec{u}_b = \vec{u}_w + \vec{u}_c \qquad (2)$$

The self-motion velocity of microorganisms was assumed to be an exponential change in nutrient concentration:

$$\vec{u}_c = K_c\nabla(\ln C_s) \qquad (3)$$

where K_c is chemotactic coefficient.

The dispersion of microorganisms in the aqueous phase was a physical dispersion phenomenon, so it could be expressed by the total diffusion tensor considering the existence of molecular diffusion and mechanical dispersion.[19,20]

$$\overrightarrow{D_{bw}} = \begin{bmatrix} D_{bw,xx} & D_{bw,xy} & D_{bw,xz} \\ D_{bw,yx} & D_{bw,yy} & D_{bw,yz} \\ D_{bw,zx} & D_{bw,zy} & D_{bw,zz} \end{bmatrix} \tag{4}$$

The migration of nutrients in porous media was also mainly affected by capillary force, dispersion force, and viscous force, and the nutrients are also consumed by microbes during the migration process. According to the equation of matter equilibrium, the migration equations of nutrients could be written as:

$$\frac{\partial}{\partial t}\left(\frac{\phi S_w}{B_w}C_s\right) + \frac{\partial}{\partial t}\left(\frac{\phi a s C_s}{1 + b_s C_s}\right)$$
$$= -\nabla\left(\frac{\vec{u}_w}{B_w}C_s\right) + \nabla\left(\frac{\phi S_w}{B_w}\vec{D}_{sw}\nabla C_s\right) + \frac{q_w}{V_0}C_s$$
$$- \frac{\phi S_w}{B_w Y_{b/s}}(v_{bf} + v_{bs}) - \left(\sum_{p=1}^{NP}\frac{\phi S_w v_p}{B_w Y_{p/s}}\right)$$
$$- \frac{\phi S_w m_s}{B_w}(C_b + \sigma C_{bs}) \tag{5}$$

The metabolites could be dissolved in the aqueous phase and adsorbed on the pore surface in the process of transport in porous media. According to the equation of matter equilibrium, the migration equations of metabolites could be written as:

$$\frac{\partial}{\partial t}\left(\frac{\phi S_w}{B_w}C_p\right) + \frac{\partial}{\partial t}\left(\frac{\phi a_p C_p}{1 + b_p C_p}\right)$$
$$= -\nabla\left(\frac{\vec{u}_w}{B_w}C_p\right) + \nabla\left(\frac{\phi S_w}{B_w}\vec{D}_{pw}\nabla C_p\right) + \frac{q_w}{V_0}C_p$$
$$+ \frac{\phi S_w \mu_{pm}}{B_w}\left(\frac{C_s - C_{sc}}{K_{p/s} + C_s - C_{sc}}\right)(C_b + \sigma C_{bs}) \tag{6}$$

4.2. Growth and Metabolism Equation of the Microbial System.

Based on the Monod model, the growth and metabolism equation was verified and improved by experiments considering the effect of metabolites on the growth of microorganism as:

$$\mu = \mu'_{max}\frac{C_1}{(K_{C_1} + C_1)\cdot(1 + S_1/K_{S_1})}\cdot$$
$$\frac{C_2}{(K_{C_2} + C_2)\cdot(1 + S_2/K_{S_2})}\cdots$$
$$\frac{C_m}{(K_{C_m} + C_m)\cdot(1 + S_n/K_{S_n})} \tag{7}$$

where m was the different kinds of nutrient limitation; n was the different kinds of metabolite limitation; C was the concentration of nutrients; S was the concentration of metabolites that had limitative effect on the microbial system;

μ'_{max} was maximum growth rate of microorganisms when $S = 0$; and K was the semisaturation index.

If only one kind of nutrient and metabolite had limitative effect on the microbial system, respectively, the growth and metabolism equation could be written as:

$$\mu = \mu'_{max}\frac{C_s}{(K_{C_f} + C_s)\cdot(1 + S/K_S)} \tag{8}$$

4.3. Physical Change Equations in Porous Media.

Some pores were inaccessible to microorganisms after the microbial system was injected into the porous medium, so porosity in the microbial migration equation needs to be improved as:

$$\phi = [1 - \phi(C_b)_{IPV}]\phi_0 \tag{9}$$

where ϕ was the improved porosity; ϕ_{IPV} was the non-accessible porosity; $\phi(C_b)_{IPV}$ was a function associated with the strain concentration and the function relation was obtained by experimental fitting; and ϕ_0 was the initial porosity of porous media. Because nutrients and metabolites were completely dissolved in water and the molecular size was much smaller than the pore radius, the porosity in the migration equation of nutrients and metabolites did not need to change.

The Taylor model could better describe the permeability reduction by biofilms. So, the Taylor model was used as the permeability equation:[21]

$$K = \frac{m\phi_1^{1/2}\beta^2 h_b^2}{8}\left(\frac{h_b}{R}\right)^{2\lambda}\cdot\left[I_3\left(\frac{R}{L_b} - 1, \lambda\right) - I_3\left(\frac{r}{L_b}, \lambda\right)\right]^2 \tag{10}$$

where

$$\beta = \lambda\phi\left[1 - \left(\frac{r_0}{R}\right)^{\lambda}\right]^{-1} \tag{11}$$

$$I_3(u, \lambda) = \int_0^u \frac{x^3}{(1 + x)^{3-\lambda}}dx \tag{12}$$

The interfacial tension of oil and water was changed in the process of microbial metabolism, thus affecting the capillary pressure between oil and water. The capillary pressure could be written as:

$$p_{cow} = p_{cow}^w\left(\frac{\sigma_{ow} - \sigma_{min}}{\sigma_{max} - \sigma_{min}}\right) \tag{13}$$

where p_{cow}^w was the capillary pressure between oil and water when the number of capillary was lower.

The interfacial tension between oil and water was changed when the metabolites contained a biosurfactant. The change of interfacial tension was related to the concentration of the biosurfactants as:

$$\log(\sigma_{ow}) = \log(\sigma_{min}) + \left[\log\left(\frac{\sigma_{max}}{\sigma_{min}}\right)\right]\left(\frac{C_{st,max} - C_{st}}{C_{st,max} - C_{st,min}}\right)^{e_s} \tag{14}$$

where σ_{ow} was the instantaneous interfacial tension between oil and water; σ_{min} was the minimum interfacial tension value between oil and water; σ_{max} was the maximum interfacial tension value between oil and water; C_{st} was the instantaneous

concentration of the biosurfactant; $C_{st,\,min}$ was the minimum biosurfactant concentration value; $C_{st,\,max}$ was the maximum biosurfactant concentration value; and e_s was a parameter.

The change of capillary number was related to the interfacial tension. When the interfacial tension decreased, the number of capillary increased so that the remaining oil can be activated. The residual phase saturation equation was shown as follows:

$$S_{or} = S_{or}^h + (S_{or}^w - S_{or}^h)T_{o1}[\log(N_{co}) + T_{o2}] \tag{15}$$

$$S_{wr} = S_{wr}^h + (S_{wr}^w - S_{wr}^h)T_{w1}[\log(N_{cw}) + T_{w2}] \tag{16}$$

$$T_{o1} = \left[\log\left(\frac{N_{co}^w}{N_{co}^h}\right)\right]^{-1}, \qquad T_{o2} = -\log(N_{co}^h) \tag{17}$$

$$T_{w1} = \left[\log\left(\frac{N_{cw}^w}{N_{cw}^h}\right)\right]^{-1}, \qquad T_{w2} = -\log(N_{cw}^h) \tag{18}$$

$$N_{co} = \frac{|\vec{K}\nabla\Phi_o|}{\sigma_{ow}} = \frac{\sqrt{K_x\frac{\partial\Phi_o}{\partial x} + K_y\frac{\partial\Phi_o}{\partial y} + K_z\frac{\partial\Phi_o}{\partial z}}}{\sigma_{ow}} \tag{19}$$

$$N_{cw} = \frac{|\vec{K}\nabla\Phi_w|}{\sigma_{ow}} = \frac{\sqrt{K_x\frac{\partial\Phi_w}{\partial x} + K_y\frac{\partial\Phi_w}{\partial y} + K_z\frac{\partial\Phi_w}{\partial z}}}{\sigma_{ow}} \tag{20}$$

where S_{or}^w was the residual oil saturation of the oil phase when the number of capillary tubes was low; S_{or}^h was the residual oil saturation of the oil phase when the number of capillary tubes was high; S_{wr}^w was the residual oil saturation of the water phase when the number of capillary tubes was low; S_{wr}^h was the residual water saturation of the oil phase when the number of capillary tubes was high; N_{co} was the capillary number of the oil phase; N_{cw} was the capillary number of the water phase; $\vec{K}$ was the permeability tensor; Φ_o was the oil phase potential; and Φ_w was the water phase potential.

The change of residual phase saturation could lead to the change of relative permeability. The relative permeability equation could be written as:

$$K_{ro}(S_o) = K_{ro}^w(S_o) + \frac{S_{or}^w - S_{or}}{S_{or}^w - S_{or}^h}[K_{ro}^h(S_o) - K_{ro}^w(S_o)] \tag{21}$$

$$K_{rw}(S_w) = K_{rw}^w(S_w) + \frac{S_{wr}^w - S_{wr}}{S_{wr}^w - S_{wr}^h}[K_{rw}^h(S_w) - K_{rw}^w(S_w)] \tag{22}$$

The biopolymer in the metabolites would increase the viscosity of the aqueous phase, so the viscosity of the aqueous phase was changed by the following equation:

$$\mu_{pol} = \mu_w + K_{pol}C_{sp} \tag{23}$$

where μ_w was the viscosity of the water phase without a biopolymer; C_{sp} was the concentration of biopolymers; and K_{pol} was the constant.

4.4. Black Oil Model. If the flow of a component existed in the oil phase and the water phase, the basic material balance equation of the component could be written as:[22]

$$\frac{\partial}{\partial t}\left(\varphi \sum_{l=o} x_{cl}\rho_l S_l\right) = -\nabla\left(\sum_{l=o} x_{cl}\rho_l \vec{u}_l\right) - \sum_{l=o} x_{cl}\tilde{m}_l \tag{24}$$

$$\frac{\partial}{\partial t}\left(\varphi \sum_{l=w} x_{cl}\rho_l S_l\right) = -\nabla\left(\sum_{l=w} x_{cl}\rho_l \vec{u}_l\right) - \sum_{l=w} x_{cl}\tilde{m}_l \tag{25}$$

where x_{cl} was the fraction of a component in an oil or water phase; ρ_l was the oil phase density or water phase density under reservoir conditions; S_l was the saturation of the oil phase or water phase; $\vec{u}_l$ was the Darcy velocity of the oil phase or water phase; and $\tilde{m}_l$ was the unit velocity of injection (extraction) in the oil phase or water phase.

The black oil model used in this paper only considered the existence of the oil phase and water phase, and there was no phase transition between oil and water. The pressure control equation of the oil phase and water phase was derived by the IMPES method as:

$$\varphi C_t \frac{\partial p_o}{\partial t} = \sum \beta_o\left[\nabla(\psi_o\nabla p) + GC_o - \frac{q_o}{V_b}\right] \tag{26}$$

$$\varphi C_t \frac{\partial p_w}{\partial t} = \sum \beta_w\left[\nabla(\psi_w\nabla p) + GC_w - \frac{q_w}{V_b}\right] \tag{27}$$

And the saturation of the oil and water phases was derived as:

$$\frac{\partial}{\partial t}\left(\varphi \frac{S_o}{B_o}\right) = \nabla(\psi_o\nabla p) + GC_o - \frac{q_o}{V_b} \tag{28}$$

$$\frac{\partial}{\partial t}\left(\varphi \frac{S_w}{B_w}\right) = \nabla(\psi_w\nabla p) + GC_w - \frac{q_w}{V_b} \tag{29}$$

4.5. Solution of Mathematical Models. An $N_x \times N_y \times N_z$ grid system was established. There were N_x grid units on each line, N_y grid units on each column, and N_z grid on the longitudinal direction. The sequence of lattice blocks in the system was within the line, from one line to the other, and from one plane to the other.

Because the partial differential equations established above were not easy to solve, the pressure distribution should be solved implicitly, the saturation of each phase should be solved explicitly, and then the flow velocity of the liquid phase Darcy was calculated. Finally, the migration equations of each component were solved explicitly. The LSOR algorithm was used to solve the pressure equations; the line (MOL) method[23] and three-order Runge−Kutta−Fehlberg (RKF) formula[24,25] were used to solve the component migration equation.
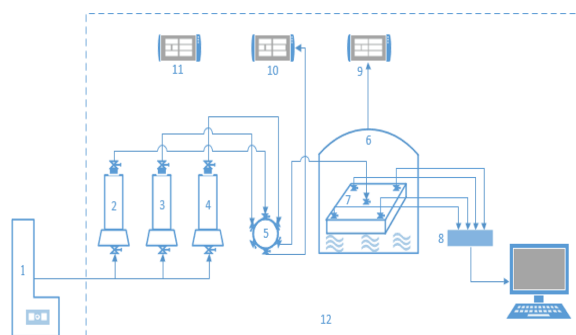
The finite difference scheme for the pressure equation could be solved as:

$$AT_z p_{z-1}^{n+1} + AS_y p_{y-1}^{n+1} + AW_x p_{x-1}^{n+1} + AB_z p_{z+1}^{n+1} + AN_y p_{y+1}^{n+1}$$
$$+ AE_x p_{x+1}^{n+1} + E_{xyz} p_{xyz}^{n+1} = B_{xyz} \tag{30}$$

The finite difference scheme for the saturation equation could be solved as:

$$S_{o,xyz}^{n+1} = \left(\frac{B_o}{V_p}\right)_{xyz}^{n+1}\left[\left(V_p\frac{S_o}{B_o}\right)^n + \Delta t(\Delta A_o \Delta p^{n+1} + GCOT - q_o)\right]_{xyz} \tag{31}$$

1- ISCO pump; 2- container for formation water; 3- container for crude oil; 4- container for microbial system; 5- Six-way valve; 6- core holding unit; 7- Three dimensional plate core; 8- Metering device for oil and water extraction; 9- pressure controller; 10- pressure monitor; 11- temperature controller; 12- dynamic simulation system of microbial flooding

Figure 12. The schematic diagram of experimental installation and procedure.

$$S_{w,xyz}^{n+1} = \left(\frac{B_w}{V_p}\right)_{xyz}^{n+1}\left[\left(V_p\frac{S_w}{B_w}\right)^n + \Delta t(\Delta A_w\Delta p^{n+1} + GCOT - q_w)\right]_{xyz}$$
(32)

The finite difference scheme for the microbial migration equation could be solved as:

$$\left(\frac{\partial C_b}{\partial t}\right)_{xyz} = \left\{\frac{1}{D_s}\left[-\nabla\left(\frac{\vec{u}_w}{B_w}C_b\right) - K_c\nabla(C_b\nabla\ln C_s)\right.\right.$$
$$+ \nabla\left(\frac{\phi S_w}{B_w}\vec{D}_{bw}\nabla C_b\right) + \frac{q_w}{V_0}C_b + \frac{\phi S_w}{B_w}v_b$$
$$\left.\left.+ \phi(v_d - v_r)\right]\right\}_{xyz}$$
(33)

The finite difference scheme for the nutrient migration equation could be solved as:

$$\left(\frac{\partial C_s}{\partial t}\right)_{xyz} = \left\{\frac{1}{D_s}\left[-\nabla\left(\frac{\vec{u}_w}{B_w}C_s\right) + \nabla\left(\frac{\phi S_w}{B_w}\vec{D}_{sw}\nabla C_s\right) + \frac{q_w}{V_0}C_s + \frac{\phi S_w}{B_w}v_s\right]\right\}_{xyz}$$
(34)

The finite difference scheme for the metabolite migration equation could be solved as:

$$\left(\frac{\partial C_p}{\partial t}\right)_{xyz} = \left\{\frac{1}{D_s}\left[-\nabla\left(\frac{\vec{u}_w}{B_w}C_p\right) + \nabla\left(\frac{\phi S_w}{B_w}\vec{D}_{pw}\nabla C_p\right) + \frac{q_w}{V_0}C_p + \frac{\phi S_w}{B_w}v_p\right]\right\}_{xyz}$$
(35)

4.6. Model Verification. To test whether the established model could simulate the oil displacement of the microbial system in the actual reservoir, the results of the indoor physical simulation experiment and numerical simulation should be verified with each other.

The core of the indoor physical simulation experiment was a three-dimensional slab casting core (size: 30 × 30 × 4.5 cm), the average permeability of the core was 100×10^{-3} μm^2, the well pattern adopted a five-point well pattern that had one injection well and four production wells, the injection system selected the CBS-2 and WBP-1 composite system that had a compound ratio of 1:1, the injection concentration was $10^5/$mL, the injection volume was 0.2 PV, and the injection speed was 1.5 mL/min. The oil and water used in experiments were all from the actual reservoir.[26] The experimental flowchart was shown in Figure 12.

MATLAB was used for numerical simulation in this paper. The five-point well pattern was simulated, where the injection well was located at the center of the model and the well was located at the corner of the model. The injection system was the same as the system used in the indoor physical simulation experiment. The first simulation was water flooding, and the simulation should be stopped when the water cut was up to 98%. The second simulation was microbial flooding, and the simulation should be stopped when the injection volume was 0.2 PV; the injection speed was 0.1 PV/a. The third simulation was follow-up water flooding, and the simulation should be stopped when the water cut was up to 98%; the injection speed was 0.1 PV/a.

■ AUTHOR INFORMATION

Corresponding Author

Jingchun Wu — *Laboratory of Enhanced Oil Recovery of Education Ministry, Northeast Petroleum University, 163318 Daqing, China*; Email: w6529@163.com

Authors

Zhao Yang — *Laboratory of Enhanced Oil Recovery of Education Ministry, Northeast Petroleum University, 163318 Daqing, China;* orcid.org/0000-0003-0991-8689

Guo Zhihua — *College of Geo-science, Northeast Petroleum University, 163318 Daqing, China*

Shi Fang — *Laboratory of Enhanced Oil Recovery of Education Ministry, Northeast Petroleum University, 163318 Daqing, China*

Hanwen Zhang — *No. 1 Chemical Production Department of Daqing Refining and Chemical Company, 163318 Daqing, China*

Zhang Miaoxin — *Laboratory of Enhanced Oil Recovery of Education Ministry, Northeast Petroleum University, 163318 Daqing, China*

Complete contact information is available at:
https://pubs.acs.org/10.1021/acsomega.1c01667

Notes

The authors declare no competing financial interest.

■ REFERENCES

(1) Gerbersdorf, S.; Wieprecht, S. Biostabilization of cohesive sediments: revisiting the role of abiotic conditions, physiology and diversity of microbes, polymeric secretion, and biofilm architecture. *Geobiology.* **2015**, *13*, 68−97.

(2) Amalia, Y. H.; Dorthe, S. P.; Sidsel, M. N.; Anna, E. L. Profiling of Indigenous Microbial Community Dynamics and Metabolic Activity During Enrichment in Molasses-Supplemented Crude Oil-Brine Mixtures for Improved Understanding of Microbial Enhanced Oil Recovery. *Appl. Biochem. Biotechnol.* **2015**, *176*, 1012−1028.

(3) Chatsungnoen, T.; Chisti, Y. Oil production by six microalgae: impact of flocculants and drying on oil recovery from the biomass. *J. Appl. Phycol.* **2016**, *28*, 2697−2705.

(4) Yang, Z.; Jingchun, W.; Fang, S. The Effect of Biofilm on Permeability of Porous Media. *Basic Clin. Pharmacol. Toxicology* **2018**, *122*, 14−28.

(5) Gunaseelan, D.; Vivek, R.; Chandrakanth, B.; Abhivyakti, D.; Susmita, D.; Kranthikiran, A.; Ramkrishna, S. Biosurfactant-biopolymer driven microbial enhanced oil recovery (MEOR) and its optimization by an ANN-GA hybrid technique. *J. Biotechnol.* **2017**, *256*, 46−56.

(6) Ke, C. Y.; Lu, G. M.; Li, Y. B.; Sun, W. J.; Zhang, Q. Z.; Zhang, X. L. A pilot study on large-scale microbial enhanced oil recovery (MEOR) in Baolige Oilfield. *Int. Biodeterior. Biodegrad.* **2018**, *127*, 247−253.

(7) Zhang, J.; Xue, Q.; Gao, H.; Lai, H.; Wang, P. Production of lipopeptide biosurfactants by Bacillus atrophaeus 5-2a and their potential use in microbial enhanced oil recovery. *Microb. Cell Fact.* **2016**, *15*, 168.

(8) Wang, Z.; Gao, D.; Fang, J. Numerical simulation of RF heating heavy oil reservoir based on the coupling between electromagnetic and temperature field. *Fuel* **2018**, *220*, 14−24.

(9) Turali, E. Y.; Simsek, S. Conceptual and 3D simulation modeling of the Sorgun hydrothermal reservoir (Yozgat,Turkey). *Geothermics.* **2017**, *66*, 85−100.

(10) Knapp, R. M.; Civan, F.; McInerney, M. J. Modeling Growth and Transport of Microorganisms in Porous Formations. *IMACS* **1988**, *3*, 676−679.

(11) Zhang, X.; Knapp, R. M.; McInerney, M. J. A Mathematical Model for Microbially Enhanced Oil Recovery Processes. *Dev. Pet. Sci.* **1993**, *39*, 171−186.

(12) Landa-Marbán, D.; Radu, F. A.; Nordbotten, J. M. Modeling and Simulation of Microbial Enhanced Oil Recovery Including Interfacial Area. *Transp. Porous Media* **2017**, *120*, 395−413.

(13) Nielsen, S. M.; Nesterov, I.; Shapiro, A. A. Microbial enhanced oil recovery-a modeling study of the potential of spore-forming bacteria. *Computat Geosci.* **2016**, *20*, 567−580.

(14) Goudarzi, A.; Delshad, M.; Kishore, K. Surfactant oil recovery in fractured carbonates: Experiments and modeling of different matrix dimensions. *J. Pet. Sci. Eng.* **2015**, *125*, 136−145.

(15) Sivasankar, P.; Kumar, G. S. Influence of pH on dynamics of microbial enhanced oil recovery processes using biosurfactant producing Pseudomonas putida: Mathematical modelling and numerical simulation. *Bioresour. Technol.* **2017**, *224*, 498−508.

(16) Hosseininooosheri, P.; Lashgari, H. R.; Sepehrnoori, K. A novel method to model and characterize in-situ bio-surfactant production in microbial enhanced oil recovery. *Fuel* **2016**, *183*, 501−511.

(17) Bao, K.; Lie, K. A.; Møyner, O.; Liu, M. Fully implicit simulation of polymer flooding with MRST. *Computat Geosci.* **2017**, *21*, 1219−1244.

(18) Cernansky, A.; Siroky, R. Deep-Bed Filtration on Filament Layers of Particles Polydispersed in Liquids. *Int. Chem. Eng.* **1985**, *25*, 364−375.

(19) Hohl, L.; Schulz, J.; Paul, N.; Kraume, M. Analysis of physical properties, dispersion conditions and drop size distributions in complex liquid/liquid systems. *Chem. Eng. Res. Des.* **2016**, *108*, 210−216.

(20) Austad, T.; Shariatpanahi, S. F.; Strand, S. Conditions for a Low-Salinity Enhanced Oil Recovery (EOR) Effect in Carbonate Oil Reservoirs. *Energy Fuels* **2012**, *26*, 569−575.

(21) Gao, X.; Kong, B.; Vigil, R. D. Comprehensive computational model for combining fluid hydrodynamics, light transport and biomass growth in a Taylor vortex algal photobioreactor: Lagrangian approach. *Bioresour. Technol.* **2017**, *24*, 523−528.

(22) Xu, J.; Guo, C.; Jiang, R.; Wei, M. Mingzhen Wei. Study on relative permeability characteristics affected by displacement pressure gradient: Experimental study and numerical simulation. *Fuel* **2016**, *163*, 314−323.

(23) Shakeri, F.; Dehghan, M. The method of lines for solution of the one-dimensional wave equation subject to an integral conservation condition. *Comput Math Appl.* **2008**, *56*, 2175−2188.

(24) Khan, U.; Ahmed, N.; Mohyud-Din, S. T.; Bin-Mohsin, B. Nonlinear radiation effects on MHD flow of nanofluid over a nonlinearly stretching/shrinking wedge. *Neural Comput Appl.* **2017**, *28*, 2041−2050.

(25) Pazner, W.; Persson, P. O. Stage-parallel fully implicit Runge-Kutta solvers for discontinuous Galerkin fluid simulations. *J. Comput. Phys.* **2017**, *335*, 700−717.

(26) Yang, Z.; Jingchun, W. Evaluation of the Effect of Microbial Combination Flooding. *Adv. Pet. Explor. Dev.* **2016**, *11*, 52−56.